D32

N79-24033

CHARGING RATES OF METAL-DIELECTRIC STRUCTURES

Carolyn K. Purvis, John V. Staskus, James C. Roche, and
Frank D. Berkopec
NASA Lewis Research Center

SUMMARY

Metal plates partially covered by 0.01-centimeter-thick fluorinated ethylene-propylene (FEP) Teflon were charged in the Lewis Research Center's geomagnetic substorm simulation facility using 5-, 8-, 10-, and 12-kilovolt electron beams. Surface voltage as a function of time was measured for various initial conditions (Teflon discharged or precharged) with the metal plate grounded or floating. Results indicate that both the charging rates and the levels to which the samples become charged are influenced by the geometry and initial charge state of the insulating surfaces.

The experiments are described and the results are presented and discussed. NASA charging analyzer program (NASCAP) models of the experiments have been generated, and the predictions obtained are described. Implications of the study results for spacecraft are discussed.

INTRODUCTION

Anomalous behavior of geosynchronous spacecraft has been attributed to the arc discharging of differentially charged spacecraft surfaces (ref. 1). In examining the response of a spacecraft to the charging environment, it is of interest to identify both the potentials to which various spacecraft surfaces charge and the rates at which these potentials vary in response to environmental changes. Of particular interest are the magnitudes and rates of change of the potential differences between various spacecraft surfaces.

It has been reported that the potentials (with respect to space plasma potential) of the ATS-5 and ATS-6 spacecraft structures can change rapidly by kilovolts in response to changes in the plasma environment, entry into and exit from eclipse, or the turning on or off of particle emitters (refs. 2 and 3). This is not surprising since the capacitance of these spacecraft with respect to the environment is small. The question of interest here is the effect of such changes on potential differences between spacecraft structures and insulating surface materials. Ground studies have shown that insulating films mounted on grounded substrates and subjected to bombardment by monoenergetic electron beams with current densities typical of the geosynchronous substorm environment require several minutes to reach equilibrium (refs. 4 and 5). Calculations with one-dimensional models indicate that even longer times may be required to develop equilibrium differential charges in the actual space environment (ref. 5).

The study described in this paper was undertaken to investigate charging rates and final potentials of insulating surfaces and underlying metal portions of composite metal-dielectric structures. It is an extension of work previously reported (ref. 5). Ideas touched on in the earlier study are refined and revised on the basis of the data presented here. This paper describes the composite samples, the experiments, and their results. Predictions of the NASCAP code (ref. 6) for some of the experiments are presented and compared with the data. Implications of the results for spacecraft are discussed.

EXPERIMENT DESCRIPTION

The experiments were performed in the Lewis Research Center's geomagnetic substorm simulation facility (ref. 7). Samples were bombarded with beams of 5-, 8-, 10-, and 12-kilovolt electrons at a current density of 1 nA/cm^2. All tests were performed in the dark.

Samples Tested

Samples consisted of metal plates of aluminum alloy partially covered by strips of 0.01-centimeter-thick silvered FEP Teflon tape in several configurations. The tape was applied to the plates, silver side down, with conductive adhesive. The plates were mounted on 6.3-centimeter-long ceramic posts to provide electrical isolation. Coaxial cable leads from the plates were brought outside the tank so that the plates could be grounded to the tank structure or allowed to float electrically.

Tests were performed on samples with four different patterns of Teflon tape, shown in figure 1. All the plates were 15.2 centimeters by 20.6 centimeters and the Teflon tape was 5 centimeters wide. In the figure, crosshatched areas (labeled M) represent exposed metal and plain areas (labeled T) represent Teflon. The Teflon area is one-third the total for configuration 1, two-thirds the total for configurations 2 and 3, and the entire surface area for configuration 4.

Test Sequences

Two series of tests were run: The first used one sample of configuration 1 and one of configuration 2, and the second used one sample each of configurations 2, 3, and 4. Test sequences and quantities measured were the same for both series of tests, but diagnostic capabilities were increased for the second series.

In the first series of tests, surface voltage data were taken with a TREK Model 340 and a surface voltage probe that was mounted on a radial arm and swept across the samples at a distance of 2 to 3 millimeters from the surface. The probe was positioned to pass across the center of the sample (series 1 probe track in fig. 1). The probe could also be stopped at any point in its sweep. Time histories of sample charging were taken both with the probe sweeping back and forth across the sample surface and with the probe stopped over the exposed metal plates. The stopped positions were chosen so that the probe's 0.95-centimeter-diameter head did not shield the Teflon from the beam.

In the second series, two TREK Model 340 HV surface voltage probes were mounted on the same swinging arm, again 2 to 3 millimeters from the surface. These probes were positioned so that the upper probe passed across the vertical centerline 4.8 centimeters above the sample center and the lower probe passed across the vertical centerline 6.6 centimeters below the sample center (series 2 probe tracks in fig. 1). Stopping the double-probe system over the exposed metal plate shielded some of the Teflon from the beam. Therefore, high-voltage leads from the plates were brought outside the tank, and a third probe arrangement was set up to monitor the plate voltages during charging. This probe monitored the plate voltages during charging both with the double probes sweeping and with them stopped well away from the sample.

All voltage data were recorded on a multichannel strip-chart recorder. The probe-arm sweep rate was set so that the probes crossed the sample in about 7 seconds. Data read from the strip chart were accurate to about ±5 percent, with a minimum error in resolution of about ±100 volts. The configuration 2 sample was tested in both test series so that effects due to differences in instrumentation could be identified.

The test sequence for each sample at each beam voltage was begun with the sample surface at zero potential (measured by the probes). The sequence consisted of the following steps:

(1) With the metal plate electrically floating, the sample was exposed to the beam and allowed to charge to equilibrium.

(2) With the beam still on, the metal plate was then grounded externally and the Teflon was allowed to charge until its surface potential reached equilibrium.

(3) Then the metal plate was electrically floated and the system allowed to charge until equilibrium was again reached.

This sequence was repeated at least twice with each sample in each series so that data could be taken with the probes sweeping and with the probes stopped. In addition, some tests were run in which fully charged floating samples were shielded from the beam during the grounding of the plates.

During the testing, particularly during the third step of the sequence, some effects were observed that were traced to nonuniformities in the electron beam or to interactions of the probes with the samples. To the extent possible, such instrumentation-related effects have been eliminated from the data reported.

EXPERIMENTAL RESULTS

In this section, test results are described and illustrated with the 5- and 8-kilovolt beam data. First, important general features of the samples' responses during the test sequence are identified in the 5-kilovolt data. Then sample responses to each step of the test sequence are considered in more detail and illustrated with the 8-kilovolt data. Except as noted, responses to the 10- and 12-kilovolt beams were qualitatively the same as those at lower beam voltages. Data points for Teflon represent probe readings at the centers of the Teflon strips. Where data from two probes were available, readings were averaged; error bars are used to indicated scatter in the data where appropriate.

The charging responses of the four test samples during the test sequence with the 5-kilovolt beam are shown in figure 2. To present the charging histories on the same time scale for comparison, the "ground plate" and "float plate" points have been plotted at 240 and 540 seconds, respectively. However, since the samples were all very nearly in equilibrium in these time frames, the illustrative value of setting the time scales equal was felt to be more important than preserving their details here.

The figure indicates several noteworthy general features of the samples' responses. First, in every instance in which rapid changes of potential occurred, the potential of the plate and that of the Teflon surface changed at nearly the same rate. That is, although absolute charging (changes in potential of the whole sample) can occur rapidly, differential charging (changes of the relative potentials of the Teflon surface and the underlying plate) takes place more slowly. This is in agreement with the concept that the rate of differential charging is controlled by the capacitance between the Teflon surface and the plate, whereas the rate of absolute charging depends on the much smaller capacitance between the sample as a whole and its surroundings. Thus, when the samples were exposed to the beam at the beginning of the sequence, the Teflon surfaces and the plates changed potential at the same rate for about the first 15 seconds. Then differential potentials began to develop. When the plates were grounded (at 240 sec in fig. 2), the differential potentials between the Teflon surfaces and the plates were maintained. The Teflon surface subsequently charged back to its equilibrium potential at a rate controlled by its capacitance to the plate. Again, when the plates were floated with the Teflon surfaces precharged (at 540 sec, in fig. 2), the initial change in plate potential was reflected in an equal change in the Teflon surface potential. In this case the Teflon surface became more negative than its equilibrium potential (overshot) and began to discharge to reestablish its equilibrium with the beam.

The second general point evident from figure 2 is that the plates charged more slowly with the Teflon precharged than with it initially uncharged. The charging rate of the plates with the Teflon precharged was affected by the relative areas of Teflon and metal exposed to the beam and, to a lesser degree, by the arrangement of the Teflon strips. Thus, the configuration 1 sample plate charged most rapidly and the configuration 4 sample plate most slowly in the third step of the test sequence.

Finally, the Teflon surfaces in these tests always took on more negative potential than did the plates. This is consistent with observations of the charging of Teflon surfaces and bare metal plates (refs. 5 and 8). It means that the polarity of differential charging studied is one in which the insulation has a more negative equilibrium potential than does the metal "structure."

In the following sections, sample responses to the three steps of the test sequence are considered individually; the 8-kilovolt beam data are used to illustrate the behavior.

Step 1

In this step, the samples were charged from an "all zero" initial condition. The Teflon surfaces and the four sample plates responded as shown in figures 3(a) and (b), respectively. During the initial 15 seconds of charging, the plates and the Teflon surfaces of each configuration charged at nearly the same rate. Furthermore, all four configurations charged at the same rate. This is not surprising since the capacitances of the samples to their surroundings were nearly equal (measured to be 200±30 pF); the rate of absolute charging is dominated by this capacity.

The time histories of charging for the Teflon surfaces of the four configurations are very similar (fig. 3(a)). All are monotonic. The equilibrium potentials of the surfaces were all about -6 kilovolts, consistent with other measurements of Teflon samples (refs. 4 and 5).

Differences among the four configurations are shown by time histories of plate charging (fig. 3(b)). The data indicate that, after 20 to 40 seconds of charging, the configuration 1 plate was the least negative, the configuration 4 plate was the most negative, and the configuration 2 and 3 plates were at the same (intermediate) potential. The configuration 4 plate remained the most negative and, at equilibrium, had a potential only slightly less negative than the overlying Teflon surface and more negative than equilibrium potentials reported for bare plates (ref. 8). Although the charging of the configuration 1, 2, and 4 plates appeared monotonic, the configuration 3 plate reached a maximum negative potential at 20 to 40 seconds. It then decayed by about 500 volts to equilibrium.

These responses can be understood qualitatively by considering the currents to each sample as a whole and to its individual components (Teflon surfaces and metal) individually and the "capacitors" being charged by these currents. Initially, each sample charged as a whole at a rate that was determined by the total current it collected and its capacitance to its surroundings. Differential potentials between the Teflon surfaces and the plates result from charging the capacitors made up of these surfaces and requires currents to each side of these capacitors. The magnitude of the current available to charge the Teflon-to-plate capacitor must depend on the relative areas of Teflon and metal exposed to the beam, on the differences between the secondary emission properties of the two materials, and on fields that can deflect the electrons.

In configuration 4, the plate had no direct access to the beam. The potential of the whole sample was driven by the net current to the Teflon surface. Because the plate could only collect "stray" currents (e.g., secondaries from the Teflon or beam electrons deflected by fields around the sample), there was essentially no current available to cause differential charging, and thus only a very small differential potential developed.

In configuration 3, the Teflon area was twice that of the metal plate exposed to the beam. Evidently, the Teflon area dominated the charging of the sample during the first 20 to 40 seconds of charging and caused the plate to "overshoot" (i.e., become more negative than) its equilibrium potential. At this point, the plate emitted more secondaries than it received primaries. This resulted in a net positive current to the plate, so that the negative potential of the plate was reduced.

If this description of the behavior of the configuration 3 sample plate is correct, it must be supposed that the configuration 2 sample plate also "overshoots" its individual equilibrium potential during the first 20 to 40 seconds of charging (since the relative areas of Teflon and exposed metal are the same for these two configurations). The fact that the configuration 2 plate does not discharge must then be due to the difference between the geometrical arrangements of the Teflon strips on the two samples. The exposed metal of configuration 2 was between the two Teflon strips, but the exposed metal of configuration 3 was on the edges of the sample. Since the Teflon surfaces were more negative than the plate, a potential barrier that prevented the secondary electrons from the plate from escaping existed in configuration 2. This implies that the final potential reached by the plate in this configuration was more negative than the "equilibrium potential" that this plate would have reached had it been exposed to the beam with no Teflon on it.

Step 2

In this step of the test sequence, the metal plates of fully charged samples (i.e., both the plates and Teflon surfaces charged as at the end of step 1) were grounded, and the Teflon was allowed to charge. Some tests were run in which the metal plates were grounded with the samples exposed to the beam, and some with the samples shielded from the beam. Shielded samples were grounded during probe sweeps and with the probes stopped away from the sample. (Sweeps were made before and after the grounding of the plates to determine the potentials.) Samples exposed to the beam were generally grounded during probe sweeps so that the Teflon surface potential could be observed as charging of the Teflon with the plate grounded began. Results are illustrated in figure 4 for a sample of configuration 3. In the figure, V_T represents the potential of the Teflon surface and V_M that of the plate before the plate is grounded. The crosshatched areas show the differential between the Teflon surface and the plate. The sample is sketched in along the abscissas to indicate its location. Figure 4(a) depicts probe traces (voltage readings across the sample) taken before and after the plate was grounded and with the sample shielded from the beam. Figures 4(b) and (c) depict traces during which the plate was grounded and with the sample shielded from and exposed to the beam, respectively. In all cases, when the plate was grounded, the differential between the Teflon surface and the underlying plate was maintained, at least on the time scale of milliseconds required for the probes to sense and adjust to the change in potential. Grounding the plate is equivalent to grounding one side of a capacitor, with the other side (in this case, the Teflon surface) open circuited; the voltage across the capacitor does not change. Even if the beam is left on during the grounding of the plate, the current to the Teflon surface is too small to change the potential across the Teflon-plate capacitor noticeably in milliseconds. As shown in figure 4(c), the Teflon surface exposed to the beam began to charge after the plate was grounded, at a rate characteristic of the Teflon-plate capacitor. Charging of the Teflon surfaces with the plates grounded proceeded as in previously reported (ref. 5) charging tests of Teflon on grounded substrates.

Step 3

In this step, the plates were allowed to float electrically (by opening the ground connection) with the Teflon surface initially charged to its equilibrium potential. As has been noted (fig. 2), the plate charged negatively, causing the Teflon surface to become more negative than its equilibrium potential. Net current to the Teflon surface became positive (electrons out) so that the Teflon-to-plate capacitor was discharging while the plate-to-surroundings capacitor was charging. That is, the differential potential between the Teflon and the plate was being reduced by net electron emission current from the Teflon while the potential of the plate with respect to its surroundings was being made more negative by net electron current to the plate.

The samples' responses to step 3 of the test sequence with the 8-kilovolt beam are illustrated in figure 5. Evidently, the most important factor in determining the rate at which each sample plate charges is the area of metal exposed to the beam (fig. 5(a)). The configuration 1 plate charged most rapidly and the configuration 4 plate most slowly at every beam voltage tested. The rate at which the plate charged, in turn, determined how large an excursion from its equilibrium potential the Teflon surface made. This can be seen from 5-kilovolt data shown in figure 2; it is demonstrated more dramatically by the 8-kilovolt data shown in figure 5(b). With an 8-kilovolt beam (and also with the 10- and 12-kV beams) the potential of the configuration 1 plate changed rapidly during the first few seconds of charging. Its potential exceeded (in magnitude) the difference between the Teflon surface potential and the beam voltage (~-2 kV) before the differential between the plate and the Teflon surface had time to change. The net result was that the Teflon surface potential exceeded the beam voltage. When this happened, the electrons from the beam no longer reached the Teflon surface and the "capacitor plate," which is the Teflon surface, was effectively open circuited. The differential between the Teflon surface and the plate was maintained during the plate's charging. Probe measurements made 15 to 30 minutes later in the test sequences showed no change in this situation. The same results were obtained for this sample with the probe sweeping across the surface and with it stationary. Clearly, this behavior cannot be expected in space, where ions and higher energy electrons preclude the possibility of a true "open circuit" situation. However, it does indicate that insulating surfaces can be driven far more negative with respect to the environment than their equilibrium potentials.

At the opposite extreme, the configuration 4 sample charged so slowly that with an 8-kilovolt beam (and also the 10- and 12-kV beams), the Teflon surface did not depart noticeably from its equilibrium potential (i.e., had maximum excursions of <100 V).

Charging rates for the plates of configuration 2 and 3 samples were intermediate between those of configurations 1 and 4. As shown in figure 5(a), the configuration 2 sample plate charged slightly faster than did the configuration 3 plate with the 8-kilovolt beam. The difference in charging rates of these two sample plates is more marked with the 5-kilovolt beam (fig. 2) but appears to decrease with increasing beam voltage (i.e., for the 10- and 12-kV beams). One can argue that the configuration 2 sample plate was expected to charge more quickly than the configuration 3 plate because of the trapping of the secondaries emitted by the plate in the configuration 2 sample. The reason for the decrease in the difference between charging rates of these two sample plates with increasing beam voltage is not clear. It might be due to the secondary yield decreasing with increasing impact energies for kilovolt primaries. This would reduce the number of secondaries available to be trapped and consequently reduce the difference between the currents to the plates in the two configurations.

The Teflon surfaces on the configuration 2 and 3 samples behaved in a similar fashion at all beam voltages tested. In each case the initial rise in plate potential caused the Teflon surface to become more negative than its equilibrium potential, and it proceeded to discharge slowly back to equilibrium as the plate charged. The plates for these samples charged slowly enough that the Teflon surface potential remained less (in magnitude) than the beam voltage by at least several hundred volts and was therefore able to discharge toward equilibrium.

NASCAP MODELS

The NASA charging analyzer program (NASCAP) is a computer code developed to calculate the charging of objects in three dimensions. The code and its capabilities are described elsewhere (refs. 6, 8, and 9). For this study, objects were defined in the code to represent the configuration 2 and 3 samples tested. Grid spacing was chosen to reflect the relative sizes of the samples and the test chamber, with the minimum number of grid points that gave a reasonable resolution on the sample. This choice and that of the time stepping option used were made to minimize computer time (rather than to maximize simulation accuracy). Simulations were run according to the "test tank" mode of code operation.

NASCAP Objects

Three objects were defined in the code for this study; they are illustrated in figure 6. Each object is composed of two metal plates that are one mesh unit thick and have one-mesh-unit spacing between them (fig. 6(a)). The "back" plate (i.e., the one farther from the electron gun) was held at ground potential during the simulation. Capacitance between the two plates was set at 200 picofarads to simulate the measured 200±30-picofarad capacity of the actual samples to their surroundings. The "front" plates that were exposed to the beam were defined to represent a bare metal plate (object 1, fig. 6(b)), and the configuration 2 and 3 samples (objects 2 and 3, figs. 6(c) and (d), respectively) described earlier. Each plate was six by eight surface cells in area and one cell thick. The grid points were 2.54 centimeters apart in the innermost mesh in the code. Thus the objects modeled were 15.2 centimeters by 20.3 centimeters, but the actual samples were 15.2 centimeters by 20.6 centimeters. The small difference in actual and modeled size should have had very little impact on the results. The bare metal plate was used to compare the behavior of plates with and without surface insulation. Teflon surface cells labeled "X" in figures 6(c) and (d) are those cells for which current and voltage information was printed during simulations. Figures 7 and 9 show the average values for these cells.

For the simulations in this study, standard NASCAP properties were used for the Teflon. The metal plates were modeled as aluminum, but with a secondary-electron emission coefficient of 2.6 and primary-electron energy to produce maximum secondary-electron yield for normal incidence of 350 electron volts to describe the yield of true secondary electrons. These choices are based on the results of a study in which the predicted and measured charging behaviors of materials were compared (ref. 8).

NASCAP runs were made to simulate the test sequences (steps 1, 2, and 3 in the section EXPERIMENT DESCRIPTION) for the configuration 2 and 3 samples with 8- and 10-kilovolt beams.

Simulation Results and Comparison with Data

Results of the NASCAP simulations of step 1 of the test sequence are shown in figure 7 for the 8-kilovolt beam case for objects 2 and 3. Data for configuration 2 and 3 samples are included for comparison. The code predicted that samples charge somewhat more slowly than the data indicate. However, overall agreement seems rather good. In particular, the potential of the object 3 plate was predicted to reach a maximum negative value and then decline in magnitude, as is observed in the data. The potential of the object 2 plate does not decline, again in agreement with observation. The code output indicates that this is due to suppression of the secondary electron emission from the plate by local fields in the case of object 2, as was surmised earlier. It was also speculated earlier that the plate may have "overshot" its equilibrium potential for these two sample configurations. This speculation is supported by the predicted charging histories of the metal plates of three objects shown in figure 8. Plates of objects 2 and 3 reached their maximum negative potentials about 600 volts larger in magnitude than their equilibrium values. Object 3 plate discharged to equilibrium potential after about 8 minutes total charging time; object 2 plate remained "too negative" as a result of trapping of secondaries. This illustrates the kind of insights into charging behavior that NASCAP can provide.

At the beginning of the simulation of step 2, the plate was grounded and the potentials were recalculated "immediately" afterwards (actually the code takes a 0.001-sec time step). Again, predictions are in accord with the data: Differential potential between the Teflon surface and the plate was maintained. Charging of the Teflon back to equilibrium proceeded as expected. Again, the code predicted charging to occur more slowly than was observed, but the discrepancy was not great.

Predictions for step 3 of the test sequence are much less satisfactory; the predicted rate of charging in this step was much less than the observed rate. This is illustrated in figure 9 for object 2 (configuration 2 data) with a 10-kilovolt beam. The reasons for this are not presently understood. It may be that simulation inaccuracies due to choices of grid size and time stepping option are increased by the presence of large fields due to the precharged Teflon surfaces. Another possibility is that portions of the physics not modeled in the code are more important in this step of the test sequence than in others.

Despite the discrepancy between observed and predicted charging rates with the Teflon precharged, the code does predict the general features of the data, that is, that the initial charging of the plate causes the Teflon surface to become more negative than its equilibrium potential and subsequently to discharge toward this potential as the plate charges.

SUMMARY OF RESULTS AND CONCLUSIONS

The charging response of composite metal-dielectric structures has been investigated experimentally and simulated with the NASCAP code. Overall, the code's predictions were in good agreement with the data, particularly considering the uncertainties in the material properties used as input (ref. 8). Discrepancies in the time response do indicate, however, that caution should be used in predicting behavior of objects with large differential potentials between adjacent surface grid points. The code's predictions can be used to provide insight into charging response. Several features of the charging response of the composite samples have interesting implications for the charging behavior of spacecraft.

Although potentials on an entire object can change rapidly in response to changes in its environment, differential potentials across thin insulators change much more slowly. The rate of absolute charging depends on the capacitance of the entire object to its environment and the net current it receives from the environment. The rate of differential charging between an insulating surface and the structure beneath it depends on the capacitance between them and the net difference in currents to the two "plates" of this capacitor. The currents available to charge these various "capacitors" depend on the relative surface areas of materials available to collect current from the environment, on the properties of these materials (such as secondary emission and resistivity) and their electrical interconnection, on local fields that can trap low-energy emitted particles, and on any "artificial" sources such as particle emitters. Factors that determine these currents affect both the rates at which the various "capacitors" charge and the potentials at which equilibrium with the environment is attained.

The capacitance of the spacecraft to its environment depends on its overall size, but the capacitances of various parts of the spacecraft to one another depend on the spacecraft's construction. In general, the spacecraft-to-environment capacitance is usually orders of magnitude less than the surface-to-surface capacitances. This means that sudden changes in the potential of a spacecraft do not result in sudden large changes in potentials across thin insulation. Thus, such operations as activating an electron emitter do not present an immediate arcing hazard to thin insulation. However, if there are insulating structures on the spacecraft that have small capacitances to the structure, these will charge back to their equilibrium potentials much more quickly than the thin insulators with large capacitances to the structure. This gives rise to the possibility of generating large differential potentials between different insulating surfaces after a sudden change in spacecraft potential. Finally, forcing the structure to remain at a fixed potential relative to the environment (by emitting electrons, for example) will allow large differential potentials to build up across thin insulators on time scales of minutes or tens of minutes.

Another consequence of the disparity in charging rates in the possibility of "overshoot"; that is, surfaces can acquire potentials significantly more negative (with respect to their environment) than equilibrium calculations would indicate. This is expected when there is an abrupt change in the environment of a precharged spacecraft. From an operational point of view, this effect should only be hazardous if the absolute spacecraft potential is of concern; for example, if two spacecraft are attempting to rendezvous.

From the point of view of the experimenter seeking to measure the plasma environment, both absolute and differential charging complicate the task of data interpretation. Effects of both types of charging on particle data from the ATS-5 and ATS-6 spacecraft have been reported (refs. 2, 10, and 11). Results of the present study indicate that shifts in reference potential (absolute charging) should occur relatively quickly in response to environmental changes but that changes in local fields around the spacecraft due to differential charging should occur relatively slowly. The latter effects are more subtle and thus should be more difficult to identify and eliminate in data analysis. Care should be used in locating such experiments on spacecraft and in designing scientific spacecraft to minimize charging effects.

REFERENCES

1. Rosen, A.: Spacecraft Charging: Environment-Induced Anomalies. AIAA Paper 75-91, Jan. 1975.

2. DeForest, S. E.: Spacecraft Charging at Geosynchronous Orbit. J. Geophys. Res., vol. 77, no. 4, Feb. 1, 1972, pp. 651-659.

3. Purvis, C. K.; Bartlett, R. O.; and DeForest, S. E.: Active Control of Spacecraft Charging on ATS-5 and ATS-6. Proceedings of the Spacecraft Charging Technology Conference. C. P. Pike and R. R. Lovell, eds., NASA TM X-73537, 1977, pp. 107-120.

4. Stevens, N. J.; et al.: Testing of Typical Spacecraft Materials in a Simulated Substorm Environment. Proceedings of the Spacecraft Charging Technology Conference, C. P. Pike and R. R. Lovell, eds., NASA TM X-73537, 1977, pp. 431-457.

5. Purvis, Carolyn K.; Steven, N. John; and Oglebay, Jon C.: Charging Characteristics of Materials: Comparison of Experiment Results with Simple Analytical Models. Proceedings of the Spacecraft Charging Technology Conference, C. P. Pike and R. R. Lovell, eds., NASA TM X-73537, 1977, pp. 459-486.

6. Katz, I.; et al.: The Capabilities of the NASA Charging Analyzer Program. Spacecraft Charging Technology - 1978. NASA CP-2071, 1979.

7. Berkopec, F. D.; Stevens, N. J.; and Sturman, J. C.: The Lewis Research Center Geomagnetic Substorm Simulation Facility. Proceedings of the Spacecraft Charging Technology Conference, C. P. Pike and R. R. Lovell, eds., NASA TM X-73537, 1977, pp. 423-430.

8. Roche, James C.; and Purvis, Carolyn K.: Comparison of NASCAP Predictions with Experimental Data. Spacecraft Charging Technology - 1978. NASA CP-2071, 1979.

9. Katz, I.; et al.: A Three-Dimensional Dynamic Study of Electrostatic Charging in Materials. (SSS-R-77-3367, Systems Science and Software; NASA Contract NAS3-20119.) NASA CR-135256, 1977.

10. DeForest, S. E.: Electrostatic Potentials Developed by ATS-5. Photon and Particle Interactions with Surfaces in Space, R. J. L. Grard, ed., D. Reidel Publishing Co. (Dordrecht), 1973, pp. 263-276.

11. Whipple, E. C., Jr.: Observation of Spacecraft Generated Electrostatic Fields in the Vicinity of the ATS-6 Satellite. AAS Paper 75-220, Aug. 1975.

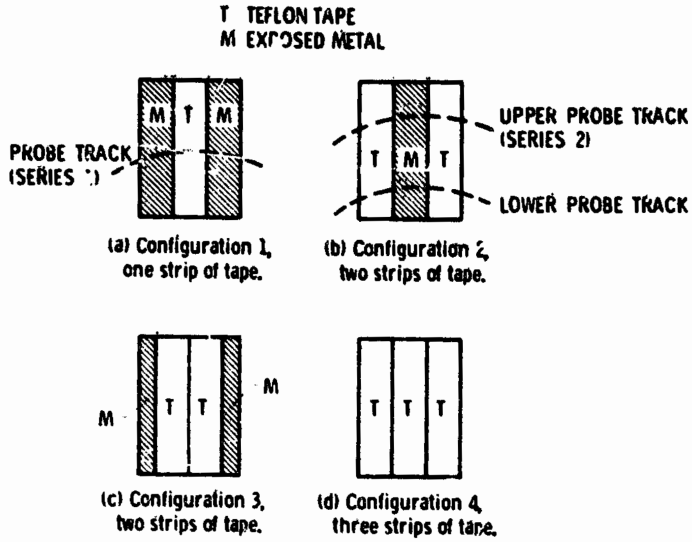

Figure 1. - Sample configurations.

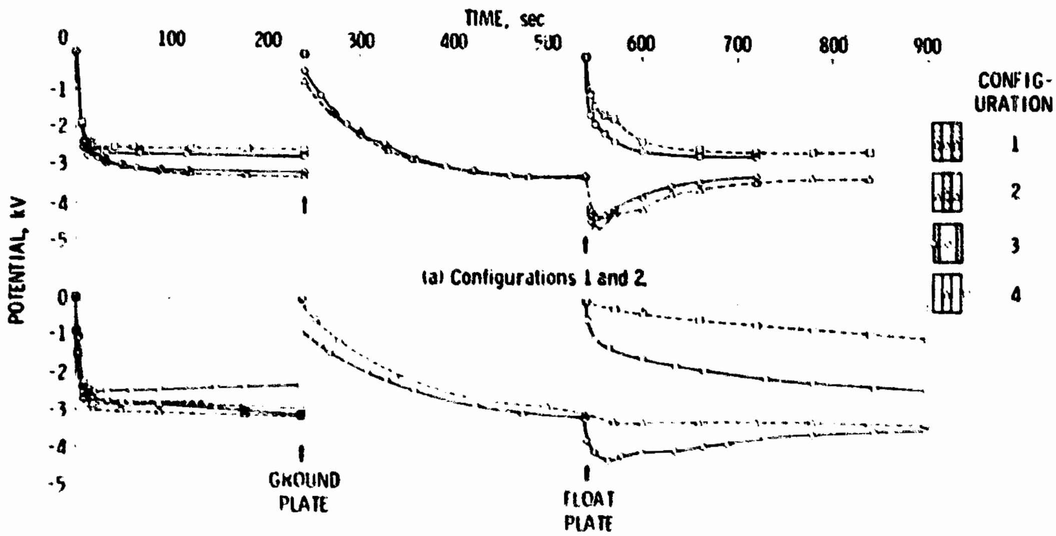

Figure 2. Charging response of samples to test sequence - 5-kilovolt beam.

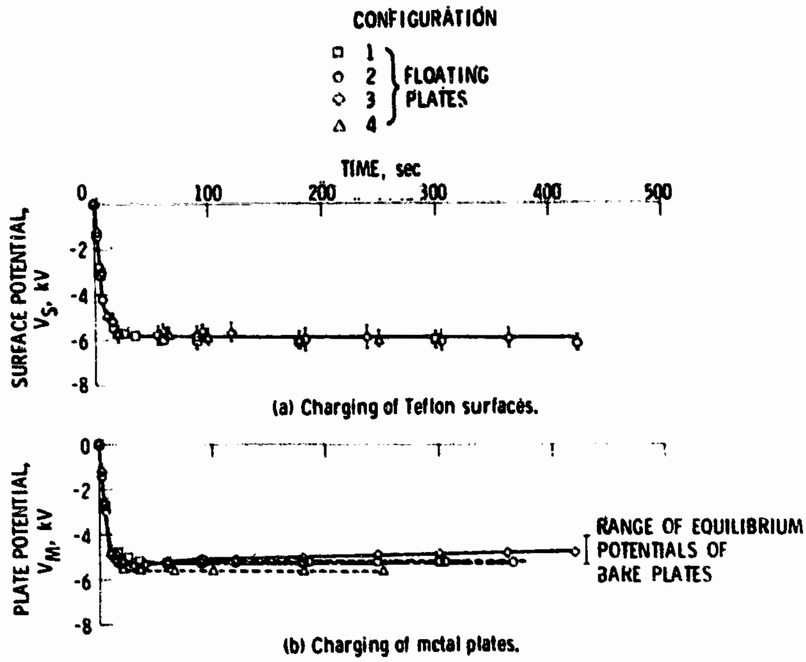

Figure 3. - Charging response of samples, sequence step 1 - 8-kilovolt beam.

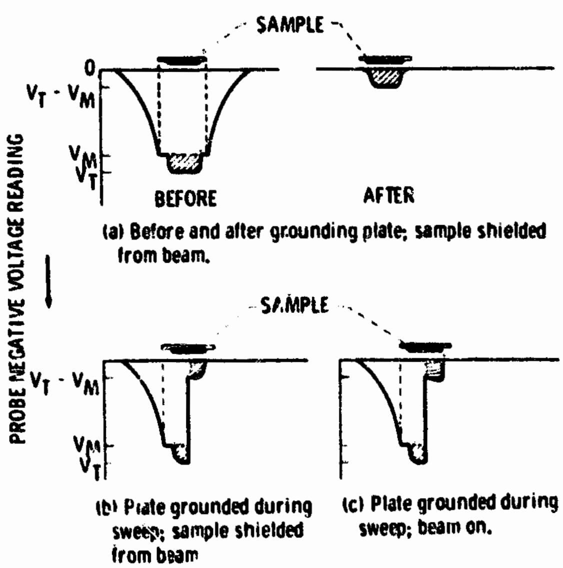

Figure 4. - Grounding of plates. Typical probe traces.

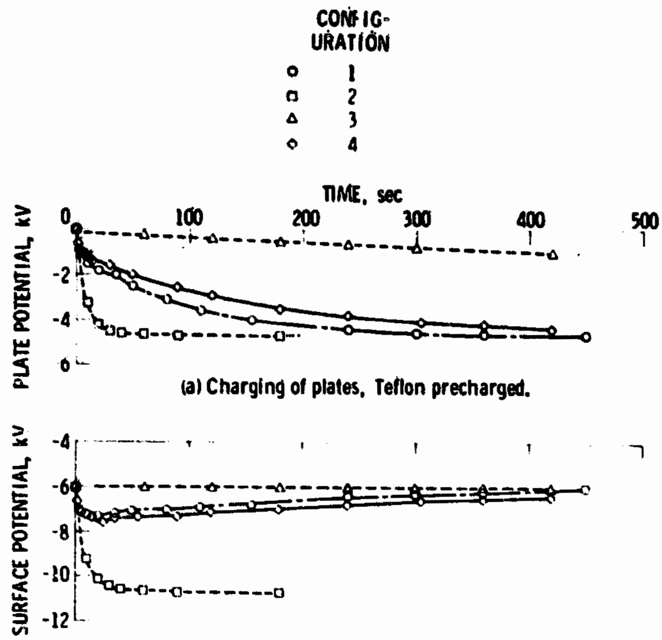

Figure 5. - Charging response of samples, sequence step 3 - 8-kilovolt beam.

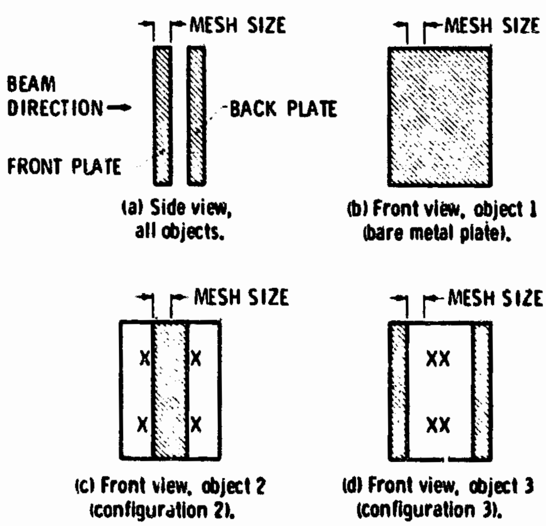

Figure 6. - NASCAP objects.

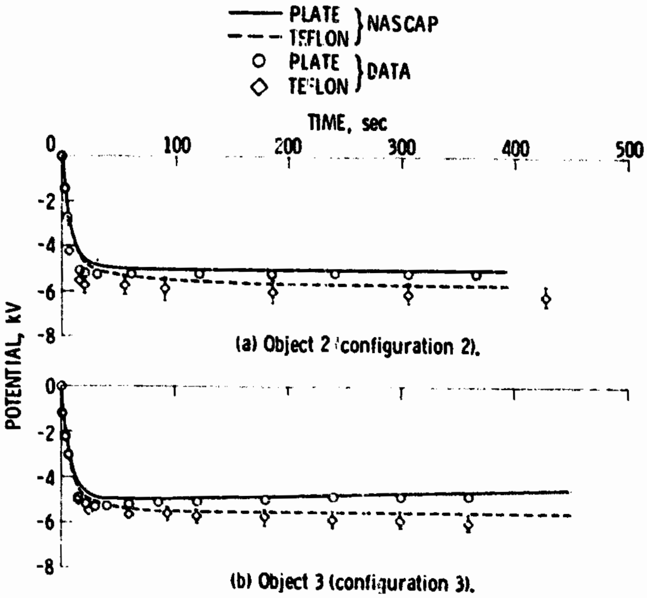

Figure 7. - Comparison of predictions with data - 8-kilovolt beam; all samples initially at zero potential.

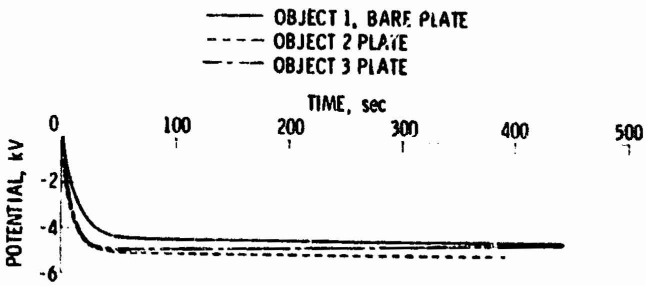

Figure 8. - NASCAP predictions, charging of metal plates - 8-kilovolt beam.

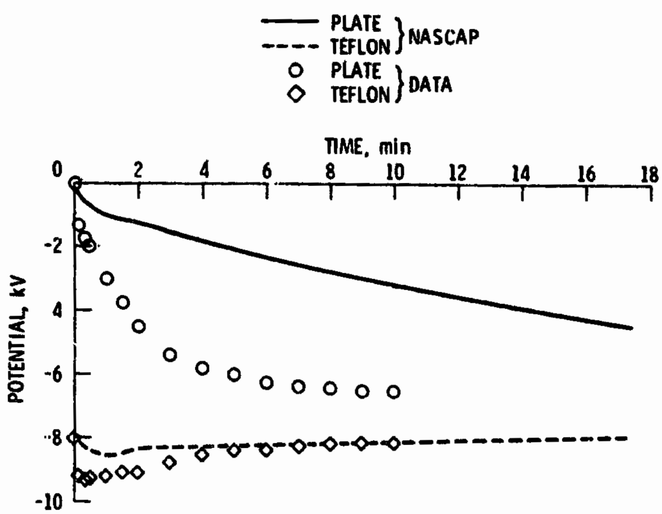

Figure 9. - Charging with Teflon precharged - 10-kilovolt beam, configuration 2.